IEEE Access
Multidisciplinary | Rapid Review | Open Access Journal

Received October 16, 2018, accepted October 25, 2018, date of publication October 30, 2018,
date of current version November 30, 2018.

Digital Object Identifier 10.1109/ACCESS.2018.2878722

Nonlinear Robust Flight Mode Transition Control for Tail-Sitter Aircraft

ZHAOYING LI[1], WENJIE ZHOU[1], HAO LIU[1,2], (Member, IEEE), LIXIN ZHANG[1], AND ZONGYU ZUO[3], (Senior Member, IEEE)

[1]School of Astronautics, Beihang University, Beijing 100191, China
[2]The University of Texas at Arlington Research Institute, The University of Texas at Arlington, Fort Worth, TX 76118, USA
[3]Department of Seventh Research Division, Beihang University, Beijing 100191, China

Corresponding author: Hao Liu (liuhao13@buaa.edu.cn)

This work was supported in part by the National Natural Science Foundation of China under Grants 61873012, 61503012, and 61673034, and in part by the Fundamental Research Funds for the Central Universities under Grants YWF-18-BJ-Y-81 and YWF-17-BJ-Y-86.

ABSTRACT In this paper, the nonlinear robust control problem for tail-sitter aircraft in flight mode transitions is addressed. The problem is challenging due to the nonlinearities and uncertainties including parametric uncertainties, unmodeled uncertainties, and external disturbances involved in the vehicle dynamics during the mode transitions. The proposed controller is designed in two steps: first, the dynamic inversion technique is adopted to establish a tracking error model; then, for the tracking error model, a robust controller consisting of a nominal controller and a robust compensator is designed. The nominal controller is designed to obtain the desired tracking performances for the nominal system. The compensator is introduced to restrain the effects of uncertainties. Tracking errors of the closed-loop system are proven to converge into a neighborhood of the origin in a finite time. Simulation results are presented to demonstrate the advantages of the proposed controller, compared with the controller based on the standard loop-shaping method.

INDEX TERMS Tail-sitter aircraft, robust control, nonlinear control, uncertainties.

I. INTRODUCTION

Over the past decades, unmanned aerial vehicles (UAVs) have drawn considerable attention due to their wide applications, such as search and rescue, reconnaissance, meteorological monitoring, and wildfire tracking, as shown in [1]. UAVs are typically classified as helicopters [2], [3], fixed-wing aircraft [4], [5], and tail-sitter aircraft [6], [7]. The tail-sitter vehicles are introduced due to their advantages of combining the vertical take-off and landing capability of the helicopters and the high forward flight speed of fixed-wing aircraft, as shown in [8]. Therefore, much interest has been aroused in the automatic control circle for the tail-sitter aircraft. Several tail-sitter aircraft flight controllers have been implemented successfully in recent years, as depicted in [9]–[13].

Many researches have been done in the past decades for designing flight mode transition controllers. In [14], a transition controller including a proportional-integral-derivative (PID) feedback controller, a feedforward controller, and controllers based on the gain scheduling approach was designed to achieve the desired tracking performances. The robust controller based on state estimator was present in [15] of nonlinear systems with parametric uncertainties and noisy outputs for quadrotor. A tracking controller based on smooth function was introduced in [16] for autonomous tail-sitter aircraft with bounded inputs. In [17], a nonlinear double integrator was introduced to obtain desired tracking performance by the acceleration measurements. In [18], an integrated altitude control design for a tail-sitter UAV equipped with turbine engines was introduced in achieving quasistationary flight. An observer was designed to reconstruct system state variables based on the system model and delayed outputs, as depicted in [19]. A controller based on the Pade approximation technique and full order observers was designed in [20]. Nonlinear controllers based on delayed-output observers were proposed in [21] to track a given reference trajectory. The influences of uncertainties were not fully considered in the stability analysis by the above-mentioned control methods.

In fact, the tail-sitter aircraft flight mode transition controller design is challenging due to the nonlinearities and uncertainties including parametric uncertainties, unmodeled uncertainties, and external disturbances. Therefore, robust control approaches have been studied to restrict the influences of these uncertainties. PID control method was adopted

in [22] to increase stability against large disturbances. In [23], the gain scheduled linear quadratic regulator (LQR) was adopted to design controllers under external disturbances. Three different transition control strategies were studied in [24] to realize the optimal transition. A control strategy based on the backstepping method was presented to perform the transition of a tail-sitter aircraft from vertical to forward flight mode in [25]. In these works, the effects of the external disturbances caused by wind and aerodynamic perturbations have been explored, but further studies on rejecting the influences of uncertainties were not sufficiently investigated.

Furthermore, studies have been done to restrict the influences of the uncertainties on the closed-loop system for the tail-sitter aircraft. In [26], a nonlinear controller was introduced with finite-time convergent observer based on Lyapunov function to estimate the unknown nonlinearities, the uncertainties, and external disturbances during mode transition. Unmodeled uncertainties and external aerodynamic disturbances were considered, but the influences of parametric uncertainties were not discussed fully in [26].

This paper aims to propose a nonlinear robust controller for flight mode transition control of the tail-sitter aircraft. The proposed controller is composite of a nonlinear controller based on the dynamic inversion technique, a linear feedback controller, and a robust compensator. The dynamic inversion technique is firstly utilized to generate a linear error model of the tail-sitter aircraft. The linear error model is considered as a nominal model with equivalent disturbances. Then, based on the tracking error model, a robust controller consisting of a nominal controller and a robust compensator is designed. The nominal controller based on the eigenvalue assignment approach is designed to obtain the desired tracking performances for the nominal system. The compensator is introduced to restrain the effects of parametric uncertainties, unmodeled uncertainties, and external disturbances.

Compared with previous studies, the proposed control method can restrain the effects of equivalent disturbances including parametric uncertainties, unmodeled uncertainties, and external disturbances. In this current paper, it is proven that if the initial conditions of the tracking states are bounded, then the tracking errors are bounded and can converge to a neighborhood of the origin in a finite time. In addition, the eigenvalue assignment method leads to linear time-invariant state feedback controllers, and it is comparatively easy to be employed in practical applications. In the current paper, a time-invariant robust controller is proposed for a time-varying nonlinear system. Furthermore, it do not need to switch the controller structure or the controller parameters for different flight status in practical applications. Therefore, the designed controller is comparatively easy to be implemented in practical applications. The simulation results show the advantages of the proposed method for improving tracking performances of the closed-loop system, compared to the loop-shaping controller.

This paper is organized as follows: the dynamic model of the tail-sitter is shown in Section II; in Section III, the nonlinear controller based on dynamic inversion technique is synthesized; in Section VI, the robust stability and the tracking properties are proven; simulation results are shown in Section V; in Section VI, conclusions are drawn.

II. TAIL-SITTER AIRCRAFT MODEL

The tail-sitter vertical take-off and landing unmanned aerial vehicle studied in this paper is developed by AOS Company called ''X-hound'', as shown in Fig. 1. The mode transition from hovering to level flight is depicted in Fig. 2. In this section, firstly, the schematic of the tail-sitter aircraft is described. Secondly, the coordinates and frames have been defined. Then, the mathematical equations of motion of the tail-sitter aircraft have been given.

FIGURE 1. X-hound aircraft.

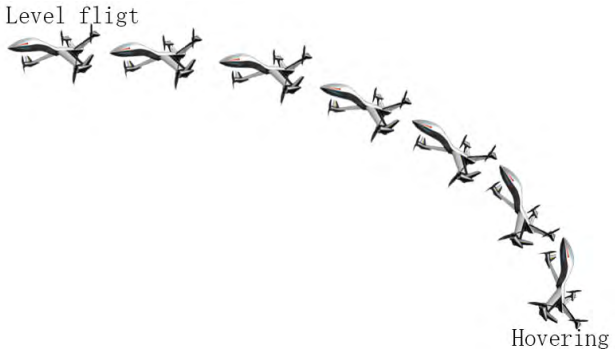

FIGURE 2. Mode transition from hovering to level.

A. SCHEMATIC OF THE TAIL-SITTER AIRCRAFT

For the tail-sitter UAV, it can be divided into three flight modes: the fly forward state, the hover state, and the mode transition. In the hover state, the tail-sitter aircraft can be regarded as a special quadrotor, and the aerodynamic analysis can be implemented based on the body fixed frame. In the fly forward state, the tail-sitter aircraft is similar to a general fixed-wing aircraft. The transition mode is similar to both the hover state and the fly forward state in some sense, and it is difficult to analyze the aerodynamic forces and torques. In this case, the body fixed frame is chosen to express the aerodynamic forces and torques in the mode transition. Therefore, to facilitate analytical calculations, the aerodynamic forces are established in the body

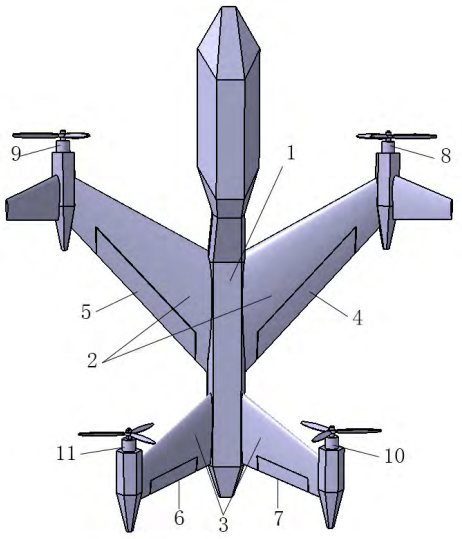

FIGURE 3. The schematic of the tail-sitter aircraft. 1: fuselage, 2: wings, 3: V-tail, 4: Vane 1, 5: Vane 2, 6: Vane 3, 7: Vane 4, 8: Rotor 1, 9: Rotor 2, 10: Rotor 3, 11: Rotor 4.

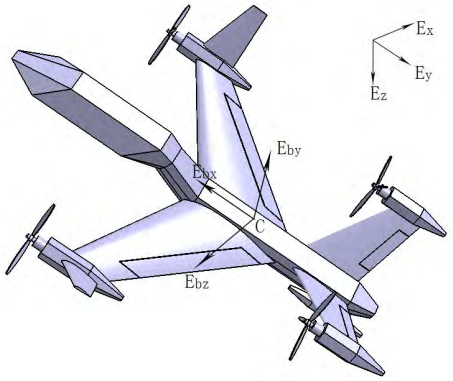

FIGURE 4. Coordinates and frames.

coordinate system. The schematic of the tail-sitter aircraft is depicted in Fig. 3. The tail-sitter aircraft consists of fuselage, two wings and V-tails as shown in Fig. 4. Thrust is generated by the propellers driven by the four motors mounted on the aircraft wings and the V-tails. Rotor 1 and Rotor 3 rotate counterclockwise, while Rotor 2 and Rotator 4 rotate clockwise. The pitch movement is achieved by the difference between the torques generated by the rotors (Rotor 1 and Rotor 2) mounted on the wings and the rotors (Rotor 3 and Rotor 4) on the V-tails. Vanes installing on wings and V-tails are utilized to generate yaw and roll movements by the deflections.

B. DEFINITION OF THE COORDINATES AND FRAMES

In Fig. 4, $E = \{E_x\ E_y\ E_z\}$ denotes an earth fixed inertial frame. $E_b = \{E_{xb}\ E_{yb}\ E_{zb}\}$ defines a body fixed frame and C is the mass center of the tail-sitter aircraft. Let $P = [x\ y\ z]^T$ be the position of the mass center of the tail-sitter aircraft relative to the inertial frame, $v = [v_x\ v_y\ v_z]^T$ denote the velocity of the mass center relative to the inertial frame, and $\omega_b = [\omega_{bx}\ \omega_{by}\ \omega_{bz}]^T$ represent the angular rates on each axis relative to the body frame. The symbol c_θ is used for $\cos\theta$ and s_θ for $\sin\theta$, the rotation matrix from the body frame to the inertial frame is expressed as follows:

$$R(\phi,\theta,\psi)=\begin{bmatrix} c_\psi c_\theta & c_\psi s_\theta s_\phi - s_\psi c_\phi & s_\psi s_\theta c_\phi + s_\psi s_\phi \\ s_\psi c_\theta & s_\psi s_\theta s_\phi + c_\psi c_\phi & s_\psi s_\theta c_\phi - c_\psi s_\phi \\ -s_\theta & c_\theta s_\phi & c_\theta c_\phi \end{bmatrix}.$$

where ϕ, θ, and ψ describe the Euler angles: the roll angle ϕ, the pitch angle θ, and the yaw angle ψ, respectively. The rotation matrix between angular rates relative to the body fixed frame and the time derivative of the attitude angles in the inertial frame is defined as follows:

$$R_v = \begin{bmatrix} 1 & 0 & -\sin\theta \\ 0 & \cos\phi & \cos\theta\sin\phi \\ 0 & -\sin\phi & \cos\theta\cos\phi \end{bmatrix}.$$

C. MATHEMATICAL MODEL

As a rigid body, the mathematical equations of motion of the tail-sitter aircraft can be derived by Newton-Euler's law and described as follows:

$$\dot{P} = v,$$
$$m\dot{v} = F_t - mgR_{be}, \quad (1)$$
$$J_t\dot{\omega}_b + \omega_b^{\times} J_t\omega_b = T_t, \quad (2)$$

where m denotes the total mass of the tail-sitter aircraft, g is the gravity constant, J_t indicates the inertial matrix of the tail-sitter aircraft, and $F_t = [F_x\ F_y\ F_z]^T$ and $T_t = [T_x\ T_y\ T_z]^T$ are the total force and torque on the aircraft in the body frame, respectively. The cross-product operation is a skew-symmetric matrix and can be defined as follows:

$$\omega_b^{\times} = S(\omega_b) = \begin{bmatrix} 0 & -\omega_{bz} & \omega_{by} \\ \omega_{bz} & 0 & -\omega_{bx} \\ -\omega_{by} & \omega_{bx} & 0 \end{bmatrix}, \quad (3)$$

and the inertial matrix J_t is given as follows:

$$J_t = \begin{bmatrix} I_x & -I_{xy} & -I_{xz} \\ -I_{xy} & I_y & -I_{yz} \\ -I_{xz} & -I_{yz} & I_z \end{bmatrix}.$$

The relationship between the angular rates and the attitude angles of the aircraft is given by the following equation:

$$\begin{bmatrix} \omega_{bx} \\ \omega_{by} \\ \omega_{bz} \end{bmatrix} = \begin{bmatrix} -\dot{\psi}\sin\theta\cos\phi + \dot{\phi}\cos\theta \\ \dot{\psi}\sin\phi + \dot{\theta} \\ \dot{\psi}\cos\phi\cos\theta + \dot{\phi}\sin\theta \end{bmatrix},$$

The total force F_t contains the thrust F_r produced by the four rotors, the aerodynamic force F_w generated by the fixed wings, and the force F_d including uncertainties and external disturbances. The total force F_t can be obtained by transforming the forces expressed in the body frame above as follows:

$$F_t = R_{be}(F_r + F_w + F_d). \quad (4)$$

The aerodynamic force F_w has the following expression:

$$F_w = \begin{bmatrix} F_{wx} \\ F_{wy} \\ F_{wz} \end{bmatrix} = \begin{bmatrix} \rho \|v\|_2^2 SC_D/2 \\ \rho \|v\|_2^2 SC_S/2 \\ \rho \|v\|_2^2 SC_L/2 \end{bmatrix}, \tag{5}$$

where ρ indicates the reference atmospheric density, $\|v\|_2 = \sqrt{v_x^2 + v_y^2 + v_z^2}$ the reference speed of the aircraft, and S the reference aircraft pneumatic area, respectively. C_D, C_S, and C_L denote, respectively, the drag force aerodynamic coefficient, the side force aerodynamic coefficient, and the lift force aerodynamic coefficient. The total torque T_t mainly consists of the aerodynamic torque T_a produced by the four vanes, the torque T_r generated by the four rotors, and the torque $T_d = \begin{bmatrix} T_{dx} & T_{dy} & T_{dz} \end{bmatrix}^T$ caused by the uncertainties and external disturbances. It can be written as follows:

$$T_t = T_a + T_r + T_d. \tag{6}$$

The aerodynamic moment T_a can be modeled as follows:

$$T_a = \begin{bmatrix} T_{ax} \\ T_{ay} \\ T_{az} \end{bmatrix} = \begin{bmatrix} \rho \|v\|_2^2 cSC_R/2 \\ \rho \|v\|_2^2 cSC_M/2 \\ \rho \|v\|_2^2 cSC_N/2 \end{bmatrix}, \tag{7}$$

where C_R, C_M, and C_N denote the aerodynamic coefficients. The torque T_r produced by the four rotors is shown as follows:

$$T_r = \begin{bmatrix} T_{rx} \\ T_{ry} \\ T_{rz} \end{bmatrix} = \begin{bmatrix} 0 \\ F_{r1}l_1 + F_{r2}l_2 - F_{r3}l_3 - F_{r4}l_4 \\ -F_{r1}l_1 + F_{r2}l_2 + F_{r3}l_3 - F_{r4}l_4 \end{bmatrix}, \tag{8}$$

where $F_{ri}\,(i = 1, 2, 3, 4)$ are the thrusts produced by the four rotors, $l_i\,(i = 1, 2, 3, 4)$ are the distances from the mass center of the tail-sitter aircraft to the center of the $i{-}th\,(i = 1, 2, 3, 4)$ rotor. The four rotors are symmetrically mounted to avoid the roll torque caused by the rotors, because these moments act in the opposite direction relative to the rotation rate of the rotor and thereby the roll torque from each rotor can be counteracted. As shown in Fig. 5, it can be obtained the position of the each rotor and the direction of the torque. Furthermore, it can be seen that the force generated by the rotor is parallel to the axis B_x in the body fixed frame as the mounted angle error neglected. According to the relationship between the wings and the fuselage, the expression of the vector r can be obtained, which determines the distance and direction of each rotor. Because the vector F_r and r are obtained, the direction of the torque can be given which is corresponding to the axis in T_r. The force generated by the four rotors are given by

$$F_{ri} = k_{ri}\omega_i^2, \quad i = 1, 2, 3, 4, \tag{9}$$

where $k_{ri}\,(i = 1, 2, 3, 4)$ define the force coefficients of rotors, and $\omega_i\,(i = 1, 2, 3, 4)$ are the angular rates of the rotors. The aerodynamic model structure adopted in the current paper is generated based on the aerodynamic database that established by the computational fluid dynamics technique at different angles of attack, sideslip angles and vane deflections conditions. The aerodynamic model is shown as follows:

$$\begin{aligned} C_D &= C_{D_0} + C_{D_\alpha}\alpha + C_{D_{\delta_a}}\delta_a + C_{D_{\delta_v}}\delta_v, \\ C_S &= C_{S_0}\beta, \\ C_L &= C_{L_0} + C_{L_\alpha}\alpha + C_{L_{\delta_a}}\delta_a + C_{L_{\delta_v}}\delta_v, \\ C_M &= C_{M_0} + C_{M_\alpha}\alpha + C_{M_{\delta_a}}\delta_a + C_{M_{\delta_v}}\delta_v, \\ C_R &= C_{R_0} + C_{R_\beta}\beta + C_{R_{\delta_a}}\delta_a + C_{R_{\delta_v}}\delta_v, \\ C_N &= C_{N_0} + C_{N_\beta}\beta + C_{N_{\delta_v}}\delta_v, \end{aligned}$$

where α, β, δ_a, and δ_v are angle of attack, sideslip angle, deflection angle of Vanes 1, 2, and Vanes 3, 4, respectively.

Unit quaternion is adopted to describe the attitude of the aircraft in order to avoid the drawback of using Euler angle which may result in the singularity problem. Simulation results are described by Euler angles to analysis the robust stability and robust tracking properties of the closed-loop systems. Quaternions have the following expressions for the given Euler angles:

$$\begin{aligned} q_0 &= \cos(\phi/2)\cos(\theta/2)\cos(\psi/2) \\ &\quad + \sin(\phi/2)\sin(\theta/2)\sin(\psi/2), \\ q_1 &= \sin(\phi/2)\cos(\theta/2)\cos(\psi/2) \\ &\quad + \cos(\phi/2)\sin(\theta/2)\sin(\psi/2), \\ q_2 &= \cos(\phi/2)\sin(\theta/2)\cos(\psi/2) \\ &\quad + \sin(\phi/2)\cos(\theta/2)\sin(\psi/2), \\ q_3 &= \cos(\phi/2)\cos(\theta/2)\sin(\psi/2) \\ &\quad + \sin(\phi/2)\sin(\theta/2)\cos(\psi/2), \end{aligned}$$

and Euler angles can be obtained by the known quaternions as shown follows:

$$\begin{aligned} \phi &= arctan\left(2(q_0q_1 + q_2q_3)/(q_0^2 - q_1^2 - q_2^2 + q_3^2)\right), \\ \theta &= arcsin\left(2(q_0q_2 - q_3q_1)\right), \\ \psi &= arctan\left(2(q_0q_3 + q_2q_1)/(q_0^2 - q_1^2 - q_2^2 + q_3^2)\right), \end{aligned}$$

then according to the given desired Euler angles, the quaternion form can be obtained. Let

$$\begin{bmatrix} q_0 & q_1 & q_2 & q_3 \end{bmatrix} = \begin{bmatrix} q_0 & q \end{bmatrix},$$

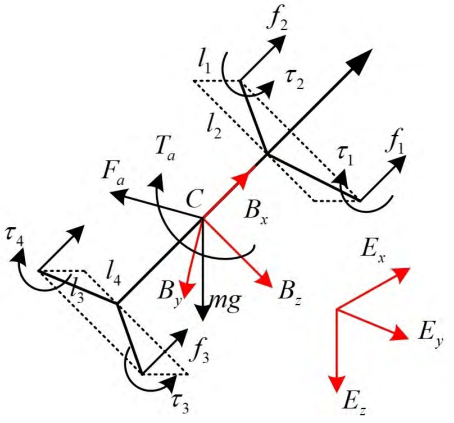

FIGURE 5. Direction of the forces and torques during the mode transition.

then the expressions can be given (see, for example, [27])

$$\begin{aligned}\dot{q} &= ((S(q) + q_0 I_3))\,\omega_b/2,\\ \dot{q}_0 &= -q^T\omega_b/2,\end{aligned} \tag{10}$$

where I_n represents an $n \times n$ identity matrix. In the current paper, the definition of the angle of attack and the sideslip angle are shown as follows:

$$\begin{aligned}\alpha &= \theta - \arctan(v_z/v_x),\\ \beta &= \arcsin\left(v_{by}/v_b\right),\end{aligned}$$

where $v_b = \sqrt{v_{bx}^2 + v_{by}^2 + v_{bz}^2}$ represents the velocity of the aircraft relative to the body frame.The tail-sitter UAV involves a large pitch maneuver during the mode transition, which may result in the stall constraint. The angle of attack is an important factor to observe the motion state of the aircraft. When the flight velocity is in a low speed state, the angle of attack may suffer from the measurement noise and therefore it is difficult to determine the aerodynamic forces and torques. Therefore, the angle of attack is defined as $\alpha = \theta - \arctan(v_{zr}/v_{xr})$ in the current manuscript, where v_{zr} and v_{xr} represent the horizontal and longitudinal velocity references in the body fixed frame. In this case, the angle of attack is equal to the pitch angle θ minus the reference trajectory angle i.e., $\arctan(v_{zr}/v_{xr})$ to avoid the drastically change during the transition mode.

Remark 1: From (5) and (7)-(9), it can be seen that there exist couplings and nonlinearities in the model of the tail-aircraft. The couplings and nonlinearities existed in the model address a challenging controller design problem for the tail-sitter aircraft.

III. NONLINEAR ROBUST CONTROLLER DESIGN

The proposed nonlinear robust control laws in the current paper consist of three parts and are designed in three steps in this section. First, a nonlinear controller based on the dynamic inversion technique is designed and is applied to counteract the known nonlinear terms to derive a linear model of the tail-sitter aircraft. Second, the eigenvalue assignment technique is applied to design a state feedback linear controller to achieve stability and desired tracking performance specifications without considering equivalent disturbances. Then, a linear robust compensator is designed for the closed-loop nominal linear system in the presence of equivalent disturbances to restrain the effects of uncertainties. Therefore, the proposed controller is composite of a nonlinear controller based on the dynamic inversion technique, a linear feedback controller, and a robust compensator.

A. NOMINAL CONTROLLER DESIGN

Nominal controllers design consist two parts: nominal attitude controller design and nominal position controller design.

A nonlinear controller based on the dynamic inversion technique is designed without taking into account the equivalent disturbances in this part. From (2) and (3), the system can be rewritten as follows:

$$\dot{\omega}_b = J_t^{-1}\left[(T_a + T_r) - \omega_b^{\times} J_t \omega_b\right]. \tag{11}$$

For the desired attitude angles ϕ_d, θ_d, and ψ_d, let $\omega_b^d = R_{be}\left[\dot{\phi}_d\ \dot{\theta}_d\ \dot{\psi}_d\right]^T$ be the given desired commands of the angular rates in the body fixed frame, where R_{be} represent the rotation matrix between the angular rates relative to the body fixed frame and the derivative of the attitude angles in the inertial frame. The tracking errors of the angular rates can be defined as follows:

$$e_{\omega_b} = \omega_b - \omega_b^d, \tag{12}$$

For the desired attitude angle ϕ_d, θ_d, and ψ_d, one can obtain the desired attitude in the quaternion expression as:

$$\begin{aligned}q_0 &= \cos(\phi/2)\cos(\theta/2)\cos(\psi/2)\\ &\quad + \sin(\phi/2)\sin(\theta/2)\sin(\psi/2),\\ q_1 &= \sin(\phi/2)\cos(\theta/2)\cos(\psi/2)\\ &\quad + \cos(\phi/2)\sin(\theta/2)\sin(\psi/2),\\ q_2 &= \cos(\phi/2)\sin(\theta/2)\cos(\psi/2)\\ &\quad + \sin(\phi/2)\cos(\theta/2)\sin(\psi/2),\\ q_3 &= \cos(\phi/2)\cos(\theta/2)\sin(\psi/2)\\ &\quad + \sin(\phi/2)\sin(\theta/2)\cos(\psi/2),\end{aligned}$$

The desired unit quaternion is $Q_d = \left[\, q_{0d}\ q_d \,\right]$ which satisfies

$$q_d^T q_d + q_{0d}^2 = 1.$$

As shown in [27], the desired unit quaternion is related to the desired angular velocity ω_b by the following dynamic equation:

$$\begin{aligned}\dot{q}_d &= ((S(q_d) + q_{0d} I_3))\,\omega_b^d/2,\\ \dot{q}_{0d} &= -q^T\omega_b^d/2.\end{aligned}$$

The angular velocity ω_b can be computed from (10) as follows:

$$\omega_b = 2(q_o\dot{q} - \dot{q}q_0) - 2S(q)\dot{q}.$$

From [36], one can obtain the quaternion tracking error as

$$\begin{aligned}e_q &= q_{0d}q - q_0 q_d + S(q)q_d,\\ e_{q0} &= q_0 q_{0d} + q^T q_d.\end{aligned}$$

Then one can rewrite (10) as follows:

$$\begin{aligned}\dot{e}_q &= ((S(q) + q_0 I_3))\,e_{\omega_b}/2,\\ \dot{e}_{q0} &= -\frac{1}{2}{e_q}^T e_{\omega_b}/2,\end{aligned} \tag{13}$$

Let $M(q) = S(q) + q_0 I_3$, then from (12), where and are tracking errors. Let , then from Eq. (12), we can rewrite the model (13) as follows:

$$\begin{aligned}\dot{e}_q &= M(q)\,e_{\omega_b}/2,\\ \dot{e}_{q0} &= -e_q^T e_{\omega_b}/2.\end{aligned} \tag{14}$$

A similar result about the formula derivation process can be seen in [27]. The position errors and the Euler angle errors

are defined as $e_i(i = 1, 2, 3, 4, 5, 6)$, where e_1, e_2, and e_3 represent the three attitude errors based on the quaternions, and e_4, e_5, and e_6 are relative to the position errors. From [35], one can obtain the attitude tracking errors e_1, e_2, and e_3 based on the quaternions as follows:

$$\begin{bmatrix} e_{a1} \\ e_{a2} \\ e_{a3} \end{bmatrix} = \Delta \times \begin{bmatrix} -q_0^r q_1 + q_1^r q_0 + q_2^r q_3 - q_3^r q_2 \\ -q_0^r q_2 - q_1^r q_3 + q_2^r q_0 + q_3^r q_1 \\ -q_0^r q_3 + q_1^r q_2 - q_2^r q_1 + q_3^r q_0 \end{bmatrix},$$
$$\Delta = 2sgn(\sum_{i=0}^{3} q_i^r q_i), \tag{15}$$

where q_i^r represent the reference quaternions signals which can be obtained by the transformation of the reference Euler angles. The position tracking errors e_4, e_5, and e_6 have the following expression:

$$\begin{bmatrix} e_{p4} \\ e_{p5} \\ e_{p6} \end{bmatrix} = \begin{bmatrix} p_1^r(t) - p_1(t) \\ p_2^r(t) - p_2(t) \\ p_3^r(t) - p_3(t) \end{bmatrix},$$

where $p_i^r(t)$ are the reference longitude position, lateral position, and vertical position signals. The Euler angle are not used to describe the attitude to avoid the singularity problem. For the nominal attitude controller design, one can define the error vector $e_a(t) = [e_{ai}(t)]_{3\times1}$. Then, e_a is the attitude tracking error vector and e_{ω_b} is rotational velocity tracking error. One can obtain that

$$\dot{e}_a = e_{\omega_b},$$
$$\dot{e}_{\omega_b} = \left(J_t^{-1}\left[(T_a + T_r) - \omega_b^{\times} J_t \omega_b\right] - \dot{\omega}_b^d\right).$$

By defining the control input as T_r, the following expression can be obtained based on the dynamic inversion technique as:

$$T_r = \omega_b^{\times} J_t \omega_b + J_t \dot{\omega}_b^d - T_a + J_t u_a.$$

where $u_a = [u_{ai}]_{3\times1}$ is virtual control input that can be adopted for the linear systems generated by the dynamic inversion technique. Therefore, one can obtain the following expression:

$$\ddot{e}_a = [u_{ai}]_{3\times1}. \tag{16}$$

Remark 2: It should be noted that the designed nonlinear control law based on the dynamic inversion technique is mainly utilized to counteract the nonlinear terms and coupling parts of the aircraft model to generate a linear error model. In this section, the uncertainties and external disturbances have not been considered. Quaternion tracking errors rather than Euler angle tracking errors are applied to avoid the singularity that may be caused by Euler angle in the mode transition process.

As for the nominal position controller design, one can define the error vector $e_p(t) = \left[e_{pi}(t)\right]_{3\times1}$, which represent the position tracking error vector. Then it can be obtained following expression:

$$\dot{e}_p = e_v,$$
$$\dot{e}_v = \left(R_{be}\left(F_r + F_w + F_d\right)/m\right) - gE_z - \dot{v}_b^d, \tag{17}$$

where e_v is the velocity tracking error and v_b^d represent the reference velocity in the body fixed frame. Let the total thrust F_r produced by the four rotors be the control input, then the following control law is selected based on the dynamic inversion technique without taking equivalent disturbances into account:

$$F_r = m(u_p - F_w)/R_{be} + gE_z + \dot{v}_b^d,$$

where $u_p = \left[u_{pi}\right]_{3\times1}$ is virtual control input that can be adopted for the linear error systems resulting by the dynamic inversion technique:

$$\ddot{e}_p = \left[u_{pi}\right]_{3\times1}. \tag{18}$$

Actually, the dynamic system can be regarded as the nominal system utilized for designing state feedback controllers. The other unknown parts of the system dynamics are treated as a part of equivalent disturbances. Then the linear error system state-space form can be written as follows:

$$\dot{E}_i = A_i E_i + B_i u_i + d_i,$$
$$y_i = C_i E_i, \quad i = 1, 2, 3, 4, 5, 6, \tag{19}$$

where $E_i = \left[\, e_i \;\; \dot{e}_i \,\right]^T$,

$$A_i = \begin{bmatrix} 0 & 1 \\ 0 & 0 \end{bmatrix}, \quad B_i = \begin{bmatrix} 0 \\ 1 \end{bmatrix}, \quad C_i = \begin{bmatrix} 1 \\ 0 \end{bmatrix}^T, \tag{20}$$

and e_i describes the position errors and the Euler angle errors of the aircraft as:

$$\begin{bmatrix} e_1 \\ e_2 \\ e_3 \end{bmatrix} = \begin{bmatrix} \dot{e}_{a1} \\ \dot{e}_{a2} \\ \dot{e}_{a3} \end{bmatrix}, \quad \begin{bmatrix} e_4 \\ e_5 \\ e_6 \end{bmatrix} = \begin{bmatrix} \dot{e}_{p1} \\ \dot{e}_{p2} \\ \dot{e}_{p3} \end{bmatrix}.$$

d_i are equivalent disturbances including the parametric uncertainties, unmodeled uncertainties, external disturbances, and nonlinear dynamics that cannot be counteracted accurately by the dynamic inversion technique.

The designed linear control laws which can be expressed as $u_i = \left[\, u_{ai} \;\; u_{pi} \,\right]^T (i = 1, 2, 3, 4, 5, 6)$ include the state feedback controllers $u_{i,con}$ $(i = 1, 2, 3, 4, 5, 6)$ and the robust compensators $u_{i,com}$ $(i = 1, 2, 3, 4, 5, 6)$, then the virtual control laws have the following expressions:

$$u_i = u_{i,con} + u_{i,com}, \quad i = 1, 2, 3, 4, 5, 6.$$

Remark 3: It should be noted that the state feedback controllers $u_{i,con}$ $(i = 1, 2, 3, 4, 5, 6)$ are designed to guarantee the stability of the nominal plant, and the robust tracking properties of the closed-loop system when uncertainties and external disturbances are considered are guaranteed by the introduced robust compensators $u_{i,com}$ $(i = 1, 2, 3, 4, 5, 6)$.

The block diagram depicted in Fig. 6 shows the overall control system of the tail-sitter aircraft. It can be seen that the overall control system consists of two channels including attitude channel and position channel. The attitude channel is designed to guarantee the rotational dynamics for desired attitude tracking, and translational dynamics for position tracking is governed by the designed position channel controllers.

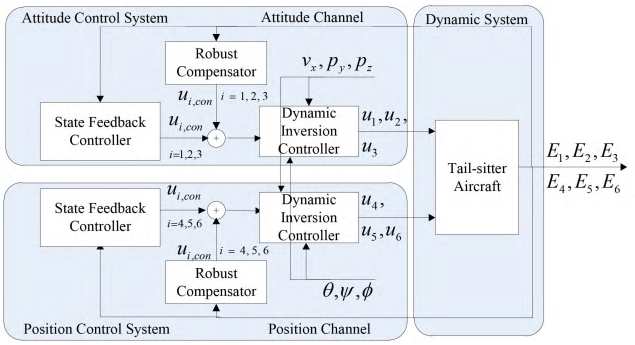

FIGURE 6. The block diagram of the robust control system.

B. STATE FEEDBACK CONTROLLER DESIGN

For linear time-invariant system, various techniques, such as linear quadratic regulation [28], eigenstructure assignment method [29]–[32], are available for designing controllers. In this paper, the widely utilized approach eigenstructure assignment method is adopted to design state feedback controllers for the linear error systems in (19). The eigenstructure assignment method is conducted by redisposing the poles of the closed-loop system with the designed controller in the s-plane. According to the given stability and performance specifications, the desired poles of the closed-loop system which determine the responses of a plant can be predetermined, and then according to the poles of the original system and the desired poles, the state feedback controllers can be designed. From (20), the linear error systems have the following forms without taking equivalent disturbances into consideration:

$$\dot{E}_i = A_i E_i + B_i u_{i,con}, \quad i = 1, 2, 3, 4, 5, 6.$$

The state feedback controllers based on the eigenvalue assignment scheme are designed with the linear error system (19), and the designed controllers based on the state feedback approach are shown as follows:

$$u_{i,con} = -K_{i,con} E_i, \quad i = 1, 2, 3, 4, 5, 6,$$

where $K_{i,con}$ $(i = 1, 2, 3, 4, 5, 6)$ are the feedback control gains determined by the eigenstructure assignment method. It can be obtained that the closed-loop systems of the plant have the desired stability and performance specifications by substituting the proposed feedback controllers into (19):

$$\dot{E}_i = \left(A_i - B_i K_{i,con}\right) E_i + B_i u_{i,con}, \quad i = 1, 2, 3, 4, 5, 6. \tag{21}$$

From (19) and (21), one can obtain that:

$$\begin{aligned} \dot{E}_i &= A_{i,con} E_i + B_i u_{i,com} + d_i, \\ y_i &= C_i E_i, \quad i = 1, 2, 3, 4, 5, 6, \end{aligned} \tag{22}$$

where $A_{i,con} = A_i - B_i K_{i,con}$ $(i = 1, 2, 3, 4, 5, 6)$. Since feedback control gains $K_{i,con}$ $(i = 1, 2, 3, 4, 5, 6)$ are properly selected to guarantee the matrices $A_{i,con}$ $(i = 1, 2, 3, 4, 5, 6)$ have eigenvalues with negative real parts, then the matrices $A_{i,con}$ $(i = 1, 2, 3, 4, 5, 6)$ are Hurwitz [34], [37]–[40].

C. ROBUST COMPENSATOR DESIGN

The state feedback control laws are designed without considering the effects of equivalent disturbances, therefore robust compensators are introduced to guarantee that the closed-loop system can achieve desired robust stability and robust tracking properties in the presence of equivalent disturbances d_i $(i = 1, 2, 3, 4, 5, 6)$.

$$G_i(s) = C_i(sI_2 - A_{i,con})^{-1} B_i, i = 1, \quad 2, 3, 4, 5, 6,$$

then the outputs of the system can be shown as bellow:

$$\begin{aligned} y_i(s) = {} & C_i(sI_i - A_{i,con})^{-1}(E_i(0) + d_i(s)) \\ & + G_i(s) v_{i,com}(s), \quad i = 1, 2, 3, 4, 5, 6. \end{aligned} \tag{23}$$

From (22) and (23), the equivalent disturbances can be counteracted if the control inputs are chosen as follows:

$$\begin{aligned} v_{i,com}(s) = {} & -G_i^{-1}(s) C_i (sI_i - A_{i,con})^{-1} d_i(s), \\ & i = 1, 2, 3, 4, 5, 6. \end{aligned} \tag{24}$$

The robust the compensators are introduced to attenuate the influence of equivalent disturbances and the following expressions deduced from (24) are given to describe the introduced robust compensators:

$$\begin{aligned} v_{i,com}(s) = {} & -F_i(s)\, G_i^{-1}(s) C_i (sI_i - A_{i,con})^{-1} d_i(s), \\ & i = 1, 2, 3, 4, 5, 6, \end{aligned} \tag{25}$$

where $F_i(s)$ $(i = 1, 2, 3, 4, 5, 6)$ are called robust filters. The robust filters $F_i(s)$ $(i = 1, 2, 3, 4, 5, 6)$ have the following expressions:

$$F_i(s) = \frac{f_i^2}{(s + f_i)^2}, \quad i = 1, 2, 3, 4, 5, 6,$$

where f_i $(i = 1, 2, 3, 4, 5, 6)$ are positive constants and determined by the specified prescribed conditions and performance specifications.

Remark 4: If f_i $(i = 1, 2, 3, 4, 5, 6)$ are sufficiently large enough, then the gains of the robust filters $F_i(s)$ $(i = 1, 2, 3, 4, 5, 6)$ are approximately equal to one and the designed compensators are asymptotic with the ideal condition, which means more effects of equivalent disturbances d_i $(i = 1, 2, 3, 4, 5, 6)$ can be counteracted.

Since the values of the equivalent disturbances cannot be measured directly, the robust compensator can be reconstructed by the following expressions:

$$\begin{aligned} d_i(s) = {} & (sI_i - A_{i,con}) E_i(s) - B_i v_{i,com}(s), \\ & i = 1, 2, 3, 4, 5, 6. \end{aligned} \tag{26}$$

From (25) and (26), the robust compensating output control laws can be expressed by the outputs y_i $(i = 1, 2, 3, 4, 5, 6)$ as shown follows:

$$\begin{aligned} v_{i,com}(s) = {} & -F_i(s)(1 - F_i(s))^{-1} G_i^{-1}(s) y_i(s), \\ & i = 1, 2, 3, 4, 5, 6. \end{aligned} \tag{27}$$

IV. ROBUST STABILITY AND TRACKING PROPERTY ANALYSIS

From (21) and (27), the linear error system can be rewritten as follows:

$$\begin{aligned} \dot{E}_i &= A_{i,con}E_i + (1 - F_i)\, d_i, \\ y_i &= C_i E_i, \quad i = 1, 2, 3, 4, 5, 6. \end{aligned} \tag{28}$$

Remark 5: Since the uncertain parameters fluctuate between lower and upper bounds, therefore, assume the parameter uncertainty terms bounded are reasonable. This is also reasonable to be applied to external disturbances.

According to [33], the equivalent disturbances are assumed to have finite norm bounds as follows:

$$\|d_i(t)\|_\infty \le \xi_{Ei}\|E_i(t)\|_\infty + \xi_i, \quad i = 1, 2, 3, 4, 5, 6,$$

where ξ_i and ξ_{Ei} $(i = 1, 2, 3, 4, 5, 6)$ are positive constants.

Remark 6: It should be noted that with the boundedness of the equivalent disturbances including parametric uncertainties, unmodeled uncertainties, and external disturbances, the robust stability and robust tracking properties of the closed-loop control system can be guaranteed. The proof has been given in the following parts.

Theorem 1: For any given positive constant ε and given bounded initial state tracking errors $E_i(0)(i = 1, 2, 3, 4, 5, 6)$, positive constants f_u and t_u can be found such that for any $f_i \ge f_u(i = 1, 2, 3, 4, 5, 6)$, the state errors $E_i(t)(i = 1, 2, 3, 4, 5, 6)$ are bounded and the output tracking errors $|y_i(t)| \le \varepsilon, \forall t \ge T_u(i = 1, 2, 3, 4, 5, 6)$ are guaranteed.

Proof: From (28), it can be obtained that

$$\begin{aligned} E(t) &= e^{A_{i,con}t}E(0) + \int_0^t e^{A_{i,con}(t-\tau)}(1 - F_i)\, d_i d\tau, \\ i &= 1, 2, 3, 4, 5, 6. \end{aligned} \tag{29}$$

From (29), it can be deduced that

$$\begin{aligned} \|E(t)\|_\infty &= \left\| e_A^t E(0) + \int_0^t e_A^{t-\tau} F_1 d_i d\tau \right\|_\infty \\ &\le \|e_A\|_\infty \|E(0)\|_\infty \\ &\quad + \left\|e_A^t\right\|_\infty \int_0^t \|e_\tau\|_\infty \|F_1\|_\infty \|d_i\|_\infty d\tau \\ &\le \|e_A\|_\infty \|E(0)\|_\infty \\ &\quad + \left\|e_A^t\right\|_\infty \int_0^t \|e_\tau\|_\infty \|F_1\|_\infty \xi_{E_i}\|E_i(t)\|_\infty d\tau \\ &\quad + \|e_A\|_\infty \int_0^t \|e_\tau\|_\infty \|F_1\|_\infty \xi_i d\tau, \\ e_A &= e^{A_{i,con}t}, \\ e_\tau &= e^{A_{i,con}-\tau}, \\ F_1 &= 1 - F_i, \\ i &= 1, 2, 3, 4, 5, 6. \end{aligned} \tag{30}$$

Let

$$-\lambda_m = maxRe(\lambda_i), \quad i = 1, 2, \tag{31}$$

where $\lambda_i < 0\,(i = 1, 2)$ indicate the eigenvalues of $A_{i,con}$ $(i = 1, 2, 3, 4, 5, 6)$ and $-\lambda_m$ is the maximum real part of the eigenvalues of $A_{i,con}$ $(i = 1, 2, 3, 4, 5, 6)$. From (31), one can obtain the following inequality:

$$\left\|e^{A_{i,con}t}\right\| \le \left\|e^{-\lambda_m t}\right\| = e^{-\lambda_m t}, \quad i = 1, 2, 3, 4, 5, 6. \tag{32}$$

From (32), one can rewrite (30) as follows:

$$\begin{aligned} \|E(t)\|_\infty &\le e^{-\lambda_m t}\|E(0)\|_\infty \\ &\quad + e^{-\lambda_m t}\int_0^t e^{-\lambda_m \tau}\|F_1\|_\infty E_\xi d\tau, \\ E_\xi &= \xi_{E_i}\|E_i(t)\|_\infty + \xi_i, \\ i &= 1, 2, 3, 4, 5, 6. \end{aligned} \tag{33}$$

The following expression can be deduced from (33):

$$\begin{aligned} e^{\lambda_m t}\|E(t)\|_\infty &\le \|E(0)\|_\infty + \int_0^t e^{-\lambda_m \tau}\|F_1\|_\infty E_\xi d\tau, \\ i &= 1, 2, 3, 4, 5, 6, \end{aligned} \tag{34}$$

then since ξ_i $(i = 1, 2, 3, 4, 5, 6)$ are positive constants, therefore, from (34), the following expression can be obtained:

$$\begin{aligned} e^{\lambda_m t}\|E(t)\|_\infty &\le \|E(0)\|_\infty \\ &\quad + \int_0^t e^{-\lambda_m \tau}\xi_{E_i}\|F_1\|_\infty \|E_i(t)\|_\infty d\tau \\ &\quad + \int_0^t e^{-\lambda_m \tau}\|F_1\|_\infty \xi_i d\tau, \\ i &= 1, 2, 3, 4, 5, 6. \end{aligned} \tag{35}$$

Since $\|1 - F_i\|_\infty$ $(i = 1, 2, 3, 4, 5, 6)$ are bounded, and ξ_i $(i = 1, 2, 3, 4, 5, 6)$ are positive constants, then the following equation can be obtained:

$$\begin{aligned} \int_0^t e^{-\lambda_m \tau}\|F_1\|_\infty \xi_i d\tau &= \|F_1\|_\infty \xi_i \int_0^t e^{-\lambda_m \tau} d\tau, \\ \|F_1\|_\infty \xi_i \int_0^t e^{-\lambda_m \tau} d\tau &= \frac{\xi_i}{\lambda_m}\|F_1\|_\infty \left(1 - e^{-\lambda_m t}\right). \end{aligned}$$

As $\lambda_m > 0$, then $\xi_i\|(1 - F_i)\|_\infty \left(1 - e^{-\lambda_m t}\right)/\lambda_m$ are bounded and let

$$m = \frac{\xi_i}{\lambda_m}\|(1 - F_i)\|_\infty \left(1 - e^{-\lambda_m t}\right), \quad i = 1, 2, 3, 4, 5, 6. \tag{36}$$

From (35) and (36), the following expression can be achieved:

$$\begin{aligned} e^{\lambda_m t}\|E(t)\|_\infty &\le \|E(0)\|_\infty + m \\ &\quad + \int_0^t e^{-\lambda_m \tau}\xi_{E_i}\|F_1\|_\infty \|E_i(t)\|_\infty d\tau, \end{aligned} \tag{37}$$

Let

$$C = \|E(0)\|_\infty + m, \tag{38}$$

then from (38), one can rewrite (37) as follows:

$$e^{\lambda_m t}\|E(t)\|_\infty \le C + \int_0^t e^{-\lambda_m \tau}\xi_{Ei}\|F_1\|_\infty \|E_i(t)\|_\infty d\tau, \tag{39}$$

According to the Bellman-Gronwall Lemma, the following conclusion can be deduced from (39):

$$e^{\lambda_m t}\|E(t)\|_\infty \le Ce^{\int_0^t \xi_{Ei}\|(1-F_i)\|_\infty d\tau}, \quad i = 1, 2, 3, 4, 5, 6, \tag{40}$$

then

$$\|E(t)\|_\infty \le Ce^{(\xi_{Ei}\|(1-F_i)\|_\infty - \lambda_m)t}, \quad i = 1, 2, 3, 4, 5, 6. \tag{41}$$

From (25), the following condition can be guaranteed when f_i $(i = 1, 2, 3, 4, 5, 6)$ are chosen large enough.

$$\xi_{Ei}\|(1-F_i)\|_\infty - \lambda_m < 0, \quad i = 1, 2, 3, 4, 5, 6. \tag{42}$$

Then it can be obtained conclusion that, for a given bounded initial tracking error $E(0)$, the tracking error $E(t)$ would be bounded if f_i $(i = 1, 2, 3, 4, 5, 6)$ are selected as $f_i \ge f_u (i = 1, 2, 3, 4, 5, 6)$.

Remark 7: It should note that the robust compensator parameters f_i $(i = 1, 2, 3, 4, 5, 6)$ are not needed to be chosen sufficiently large and can be tuned online in practical applications. The parameters f_i $(i = 1, 2, 3, 4, 5, 6)$ can be set to certain initial values to run in the whole closed-loop control systems. If the desired tracking performances are not satisfied, the parameters f_i $(i = 1, 2, 3, 4, 5, 6)$ can be reset to larger values until the desired tracking performances can be achieved.

V. SIMULATION RESULTS

The values of the nominal plant parameters are given in Table 1. The parameters of aerodynamic coefficients are shown in Table 2. Table 3 shows the values of the external disturbances, where d_{ni} $(i = 1, 2, 3, 4, 5, 6)$ indicate high frequency noise signals.

TABLE 1. Nominal parameters of the tail-sitter aircraft.

Parameters	Values	Parameters	Values
I_x	$0.263kg \cdot m^2$	I_{xy}	$6.832e^{-5}kg \cdot m^2$
I_y	$0.087kg \cdot m^2$	I_{yz}	$8.967e^{-4}kg \cdot m^2$
I_z	$0.333kg \cdot m^2$	I_{zx}	$1.548e^{-5}kg \cdot m^2$
ρ	$1.225kg \cdot m^2$	c	$1m$
S	$1m^2$		

In this paper, the process of flight mode transitions from hovering to level flight of the tail-sitter aircraft has been studied. The mode transitions require that the flight path angle changes from 90° to zero while the roll and yaw angle maintain zero. The final desired level fight velocity is set to 25 m/s and height is 30 m. Theoretically, the selected

TABLE 2. Parameters of aerodynamic coefficients.

Parameters	Values	Parameters	Values
C_{D_0}	-2.2176	C_{M_0}	0.1212
C_{D_α}	0.0295	C_{M_α}	0.1179
$C_{D_{\delta_\alpha}}$	-0.0018	$C_{M_{\delta_\alpha}}$	0.0069
$C_{D_{\delta_v}}$	0.4000	$C_{M_{\delta_v}}$	0.1309
C_{L_0}	-3.2570	C_{R_0}	-0.0509
C_{L_α}	-1.7491	C_{R_β}	-0.0233
$C_{L_{\delta_\alpha}}$	-0.1418	$C_{R_{\delta_\alpha}}$	-0.0224
$C_{L_{\delta_v}}$	0.1309	$C_{R_{\delta_v}}$	-0.0114
C_{S_0}	-1.1722	C_{N_0}	0.0083
C_{N_β}	0.0504	$C_{N_{\delta_v}}$	0.0293

TABLE 3. External disturbances.

Parameters	Values
d_1	$0.5\sin(0.001\pi t) + d_{n1}$
d_2	$0.1\sin(0.001\pi t) + d_{n2}$
d_3	$0.3\sin(0.001\pi t) + d_{n3}$
d_4	$0.1\sin(0.001\pi t) + d_{n4}$
d_5	$0.05\sin(0.001\pi t) + d_{n5}$
d_6	$0.05\sin(0.001\pi t) + d_{n6}$

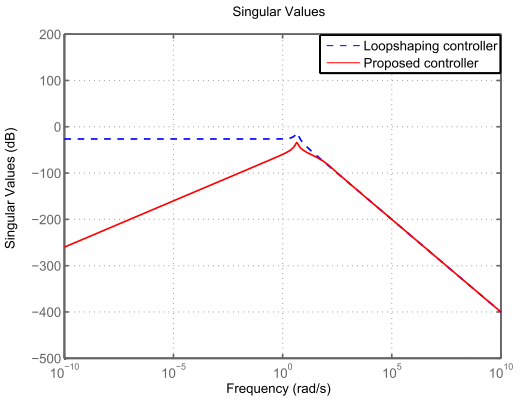

FIGURE 7. Singular values in pitch angle channel.

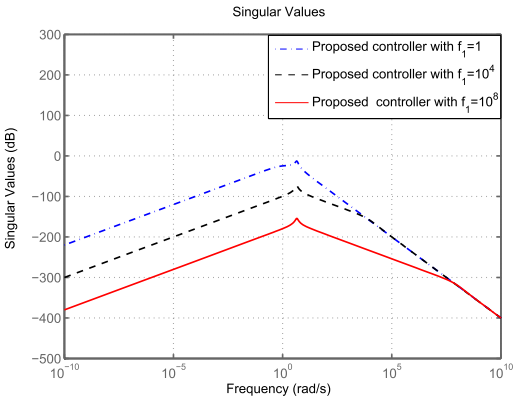

FIGURE 8. Singular values comparison in horizontal velocity channel.

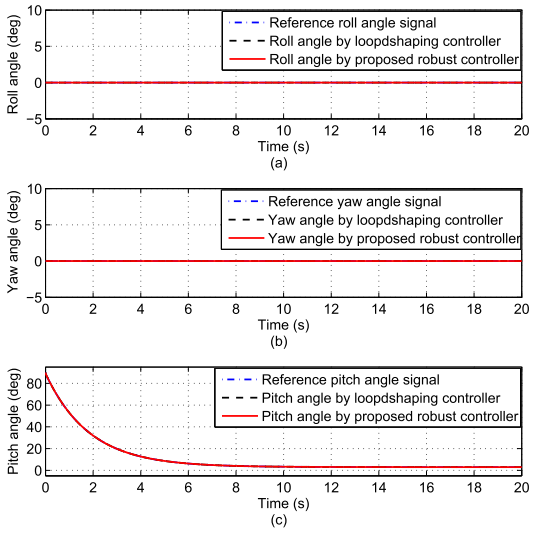

FIGURE 9. Attitude responses by loop-shaping controller and proposed controller for nominal model.

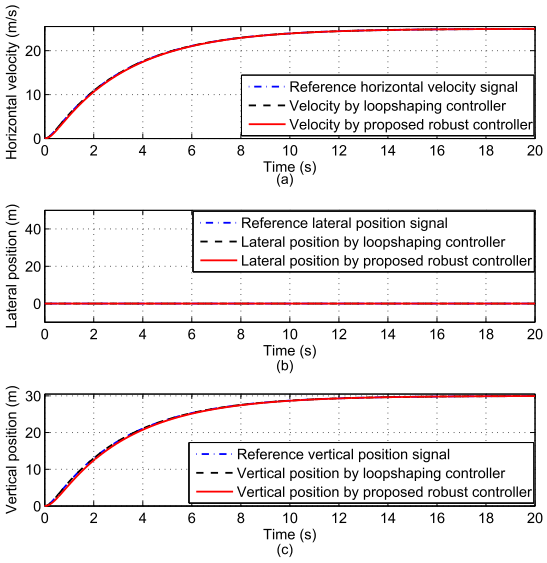

FIGURE 10. Velocity and position responses by loop-shaping controller and proposed controller for nominal model.

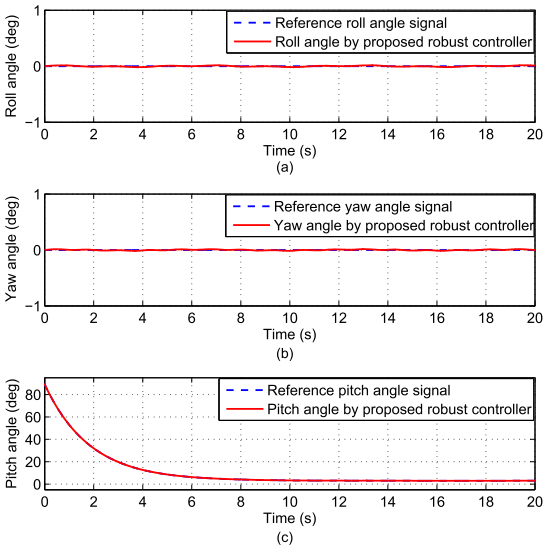

FIGURE 11. Attitude responses under uncertainties by proposed controller.

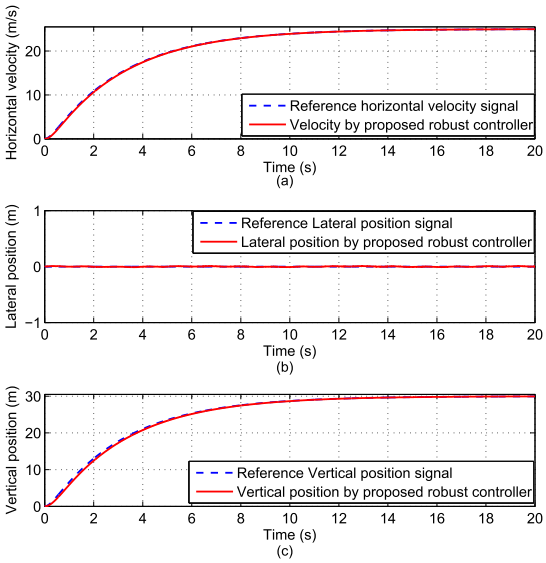

FIGURE 12. Velocity and position responses under uncertainties by proposed controller.

controller gain vectors $K_{i,con}\,(i = 1, 2, 3, 4, 5, 6)$ can guarantee the matrices $A_{i,con}\,(i = 1, 2, 3, 4, 5, 6)$ are Hurwitz. In practical design process, the gain vectors $K_{i,con}\,(i = 1, 2, 3, 4, 5, 6)$ are determined by the desired poles of the nominal closed-loop system selected based on the desired time domain performances including steady-state error, overshoot, rising time, and settling time. The desired poles of the closed-loop system are selected as

$$\begin{aligned}
\lambda_1 &= \left[\,-0.5 + 4.4j \;\; -0.5 - 4.4j\,\right],\\
\lambda_2 &= \left[\,-0.25 + 3.2j \;\; -0.25 - 3.2j\,\right],\\
\lambda_3 &= \left[\,-0.5 + 3.8j \;\; -0.5 - 3.8j\,\right],\\
\lambda_4 &= \left[\,-0.3 + 2.2j \;\; -0.3 - 2.2j\,\right],\\
\lambda_5 &= \left[-0.01 + 0.7j \;\; -0.01 - 0.7j\right],\\
\lambda_6 &= \left[\,-0.3 + 2.2j \;\; -0.3 - 2.2j\,\right].
\end{aligned}$$

Numerical simulation results of loop-shaping controllers designed based on the linearized model (22), as depicted in [34], has been shown to compare with the proposed nonlinear robust controller to demonstrate the advantages of the proposed nonlinear robust controller.

Comparison results of singular values of the closed-loop transfer functions from disturbances to the outputs in different channels are presented in Fig. 7. The results show that the singular values in low frequency of the proposed robust controllers are smaller, which means the proposed robust controllers have better properties in rejecting the disturbance effects than the loop-shaping controllers for the closed-loop system, especially in low frequency. The disturbances rejection properties of the proposed robust controllers can be improved significantly by increasing the

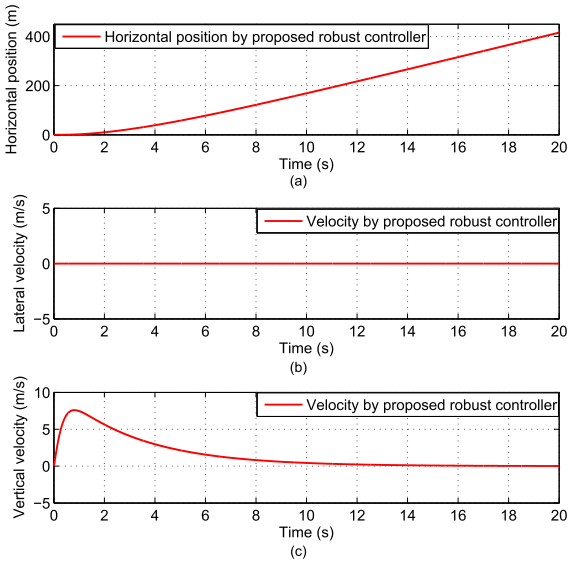

FIGURE 13. Position and velocity responses by proposed controller for nominal model.

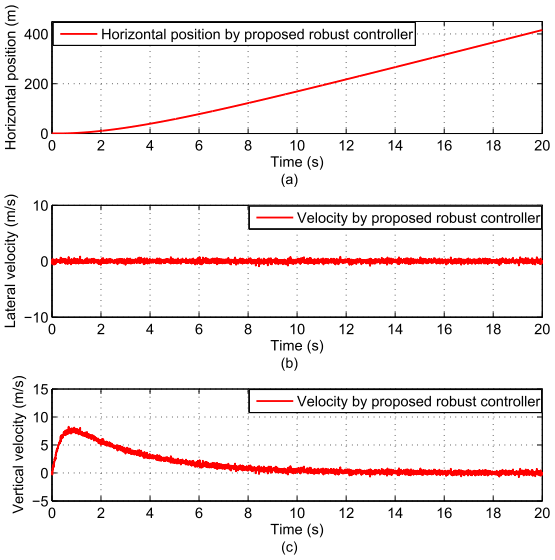

FIGURE 14. Position and velocity responses under uncertainties by proposed controller.

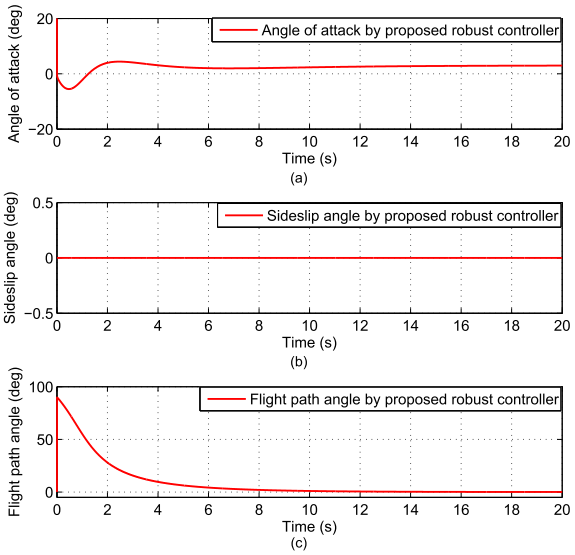

FIGURE 15. Angle of attack, sideslip angle, and flight path angle responses by proposed controller for nominal model.

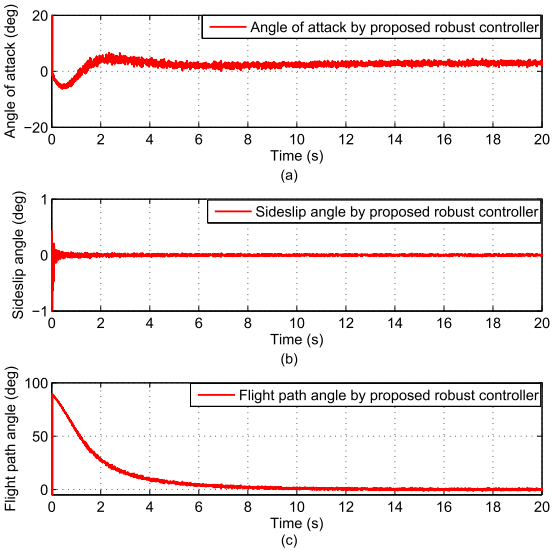

FIGURE 16. Angle of attack, sideslip angle, and flight path angle responses under uncertainties by proposed controller.

values of the f_i $(i = 1, 2, 3, 4, 5, 6)$. In Fig. 8, singular values of the closed-loop transfer functions from disturbances to the outputs with different values of f_i $(i = 1, 2, 3, 4, 5, 6)$ have been shown to demonstrate the improvement of disturbances rejection properties by increasing the values of f_i $(i = 1, 2, 3, 4, 5, 6)$.

Simulations of loop-shaping controllers and the proposed robust controllers have been conducted for the nominal nonlinear model and uncertain nonlinear model, respectively. Figs. 9-10 depict the attitude, velocity and position tracking performance responses of the nominal nonlinear model by designed loop-shaping controllers and the proposed nonlinear robust controllers. From these figures, it can be obviously obtained that both controllers can achieve desired tracking performance for the nominal nonlinear model. However, the simulation results in Figs. The uncertain nonlinear model cannot achieve desired tracking performance by the designed loop-shaping controllers when the uncertainty of the parameters are selected to be 20% larger than the nominal one while the proposed robust controllers can, as shown in Figs. 11-12. The results obviously demonstrate the advantages of the proposed controller.

Figs. 13-14 depict the movement of the horizontal position, the velocity responses of the nonlinear model in lateral direction and vertical direction with and without equivalent disturbances, respectively. It can be seen that, in Fig. 13, the nominal system of the tail-sitter aircraft is stable by the proposed robust controller. Fig. 14 shows that the response of the aircraft fluctuates in a small scope near the nominal

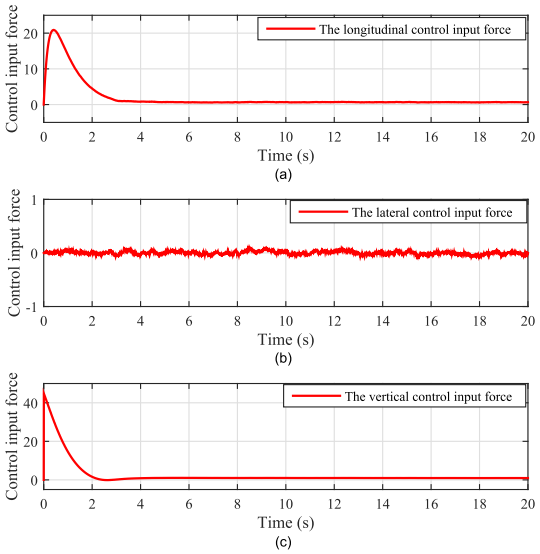

FIGURE 17. The control input force response from hover to level by proposed controller.

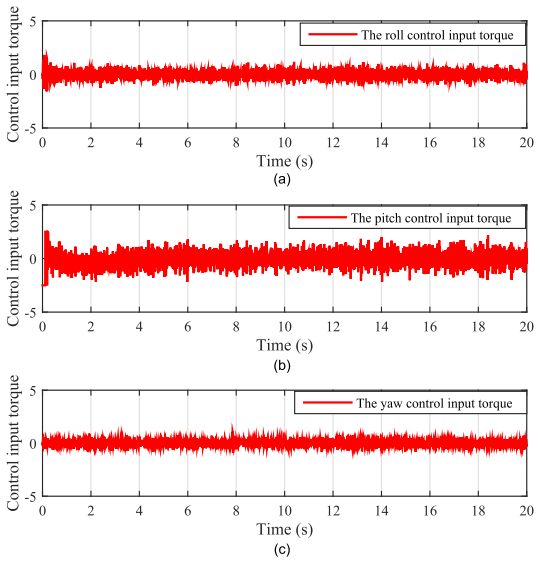

FIGURE 18. The control input torque response from hover to level by proposed controller.

response of the aircraft, which demonstrates the robustness of the proposed controller. Attack angle, slide angle and flight path angle responses in the mode transitions of the nominal nonlinear system are described in Fig. 15. Taking the uncertainties and external disturbances into account, the responses of the angle of attack, the slide angle, and the flight path angle are shown in Fig. 16. From these figures, it can be seen that the proposed robust closed-loop system of the tail-sitter aircraft can track the prescribed references. One can see the response of the control input from the proposed controller from Fig. 17 and Fig. 18, and the amplitude of the control inputs by the proposed controller is within a reasonable range.

VI. CONCLUSION

In the paper, the problem of mode transitions from hovering to level flight of a tail-sitter aircraft with external disturbances and uncertainties including parametric uncertainties, nonlinear dynamics, and unmodeled uncertainties is dealt by the proposed nonlinear robust controller. The proposed nonlinear robust controller consisting of a dynamic inversion controller, a state feedback controller, and a robust compensator can guarantee the tail-sitter aircraft can achieve desired robust stability and robust tracking properties. The proof of the robust stability and robust tracking properties has been given in this paper. The comparison simulation results are presented to show the effectiveness and advantages of proposed controller.The proof of the robust stability and robust tracking properties has been given in this paper. The comparison simulation results are presented to show the effectiveness and advantages of proposed controller.

REFERENCES

[1] Z. Xu, X. Nian, H. Wang, and Y. Chen, "Robust guaranteed cost tracking control of quadrotor UAV with uncertainties," *ISA Trans.*, vol. 69, no. 2, pp. 157–165, Jul. 2017.

[2] H. Liu, T. Ma, F. L. Lewis, and Y. Wan, "Robust formation control for multiple quadrotors with nonlinearities and disturbances," *IEEE Trans. Cybern.*, to be published, doi: 10.1109/TCYB.2018.2875559.

[3] S. Zhao *et al.*, "A robust real-time vision system for autonomous cargo transfer by an unmanned helicopter," *IEEE Trans. Ind. Electron.*, vol. 62, no. 2, pp. 1210–1219, Feb. 2015.

[4] H. Liu, W. Zhao, Z. Zuo, and Y. Zhong, "Robust control for quadrotors with multiple time-varying uncertainties and delays," *IEEE Trans. Ind. Electron.*, vol. 64, no. 2, pp. 1303–1312, Feb. 2017.

[5] B. Zhao, B. Xian, Y. Zhang, and X. Zhang, "Nonlinear robust adaptive tracking control of a quadrotor UAV via immersion and invariance methodology," *IEEE Trans. Ind. Electron.*, vol. 62, no. 5, pp. 2891–2902, May 2015.

[6] R. Naldi, M. Furci, R. G. Sanfelice, and L. Marconi, "Robust global trajectory tracking for underactuated VTOL aerial vehicles using inner-outer loop control paradigms," *IEEE Trans. Autom. Control*, vol. 62, no. 1, pp. 97–112, Jan. 2017.

[7] X. Hou and R. Mahony, "Dynamic kinesthetic boundary for haptic teleoperation of VTOL aerial robots in complex environments," *IEEE Trans. Syst., Man, Cybern., Syst.*, vol. 46, no. 5, pp. 694–705, May 2016.

[8] K. Kita, A. Konno, and M. Uchiyama, "Hovering control of a tail-sitter VTOL aerial robot," *J. Robot. Mechatron.*, vol. 21, no. 2, pp. 277–283, 2009.

[9] F. Lin, W. Zhang, and R. D. Brandt, "Robust hovering control of a PVTOL aircraft," *IEEE Trans. Control Syst. Technol.*, vol. 7, no. 3, pp. 343–351, May 1999.

[10] R. H. Stone, "The T-wing tail-sitter unmanned air vehicle: From design concept to research flight vehicle," *Proc. Inst. Mech. Eng., G, J. Aerosp. Eng.*, vol. 218, no. 6, pp. 417–433, 2006.

[11] J. Escareno, S. Salazar, and R. Lozano, "Modelling and control of a convertible VTOL aircraft," in *Proc. 45th IEEE Conf. Decis. Control*, San Diego, CA, USA, Dec. 2006, pp. 69–74.

[12] J. Hauser, S. Sastry, and G. Meyer, "Nonlinear control design for slightly non-minimum phase systems: Application to V/STOL aircraft," *Automatica*, vol. 28, no. 4, pp. 665–679, 1992.

[13] P. Martin, S. Devasia, and B. Paden, "A different look at output tracking: Control of a VTOL aircraft," *Automatica*, vol. 32, no. 1, pp. 101–107, 1996.

[14] K. Kita, A. Konno, and M. Uchiyama, "Transition between level flight and hovering of a tail-sitter vertical takeoff and landing aerial robot," *Adv. Robot.*, vol. 24, nos. 5–6, pp. 763–781, 2010.

[15] J. A. Meda-Campaña, "On the estimation and control of nonlinear systems with parametric uncertainties and noisy outputs," *IEEE Access*, vol. 6, pp. 31968–31973, 2018.

[16] A. Ailon, "Simple tracking controllers for autonomous VTOL aircraft with bounded inputs," *IEEE Trans. Autom. Control*, vol. 55, no. 3, pp. 737–743, Mar. 2010.
[17] X. Wang, "Takeoff/landing control based on acceleration measurements for VTOL aircraft," *J. Franklin Inst.*, vol. 350, no. 10, pp. 3045–3063, 2013.
[18] H. Li, C. Li, H. Li, Y. Li, and Z. Xing, "An integrated altitude control design for a tail-sitter UAV equipped with turbine engines," *IEEE Access*, vol. 5, pp. 10941–10952, 2017.
[19] Q. He and J. Liu, "An observer for a velocity-sensorless VTOL aircraft with time-varying measurement delay," *Int. J. Syst. Sci.*, vol. 47, no. 3, pp. 652–661, 2015.
[20] S. Su and Y. Lin, "Output tracking control for a velocity-sensorless VTOL aircraft with measurement delays," *Int. J. Syst. Sci.*, vol. 46, no. 5, pp. 885–895, 2015.
[21] X. Wang, J. Liu, and K.-Y. Cai, "Tracking control for a velocity-sensorless VTOL aircraft with delayed outputs," *Automatica*, vol. 45, no. 12, pp. 2876–2882, 2009.
[22] T. Matsumoto *et al.*, "A hovering control strategy for a tail-sitter VTOL UAV that increases stability against large disturbance," in *Proc. IEEE Int. Conf. Robot. Automat.*, Anchorage, AL, USA, May 2010, pp. 54–59.
[23] R. H. Stone, P. Anderson, C. Hutchison, A. Tsai, P. Gibbens, and K. C. Wong, "Flight testing of the T-wing tail-sitter unmanned air vehicle," *J. Aircrafts*, vol. 45, no. 2, pp. 673–685, 2008.
[24] A. Oosedo, S. Abiko, A. Konno, and M. Uchiyama, "Optimal transition from hovering to level-flight of a quadrotor tail-sitter UAV," *Auto. Robots*, vol. 41, no. 5, pp. 1143–1159, 2017.
[25] J. Escareño, R. H. Stone, A. Sanchez, and R. Lozano, "Modeling and control strategy for the transition of a convertible tail-sitter UAV," in *Proc. Eur. Control Conf.*, Kos, Greece, Jul. 2007, pp. 3385–3390.
[26] X. Wang, Z. Chen, and Z. Yuan, "Modeling and control of an agile tail-sitter aircraft," *J. Franklin Inst.*, vol. 352, no. 12, pp. 5437–5472, 2015.
[27] J. T.-Y. Wen and K. Kreutz-Delgado, "The attitude control problem," *IEEE Trans. Autom. Control*, vol. 36, no. 10, pp. 1148–1162, Oct. 1991.
[28] H. Liu, D. Li, Z. Zuo, and Y. Zhong, "Robust three-loop trajectory tracking control for quadrotors with multiple uncertainties," *IEEE Trans. Ind. Electron.*, vol. 63, no. 4, pp. 2263–2274, Apr. 2016.
[29] M. N. Dao, D. Noll, and P. Apkarian, "Robust eigenstructure clustering by non-smooth optimisation," *Int. J. Control.*, vol. 88, no. 8, pp. 1441–1455, 2015.
[30] J. de Jesus Rubio, E. Garcia, C. A. Ibanez, and C. Torres, "Stabilization of the robotic arms," *IEEE Latin Amer. Trans.*, vol. 13, no. 8, pp. 2567–2573, Aug. 2015.
[31] M. Huang, X. Wang, and Z. Wang, "Multiple model self-tuning control for a class of nonlinear systems," *Int. J. Control.*, vol. 88, no. 10, pp. 1984–1994, 2015.
[32] Z. Li, W. Zhou, and H. Liu, "Nonlinear robust control of hypersonic aircrafts with interactions between flight dynamics and propulsion systems," *ISA Trans.*, vol. 64, no. 2, pp. 1–11, 2016.
[33] H. Liu, J. Xi, and Y. Zhong, "Robust attitude stabilization for nonlinear quadrotor systems with uncertainties and delays," *IEEE Trans. Ind. Electron.*, vol. 64, no. 7, pp. 5585–5594, Jul. 2017.
[34] H. Liu, X. Wang, and Y. Zhong, "Quaternion-based robust attitude control for uncertain robotic quadrotors," *IEEE Trans. Ind. Informat.*, vol. 11, no. 2, pp. 406–415, Apr. 2015.
[35] K. Zhou, J. C. Doyle, and K. Glover, *Robust and Optimal Control*. Upper Saddle River, NJ, USA: Prentice-Hall, 1995, pp. 217–221.
[36] D. Braganza, W. E. Dixon, D. M. Dawson, and B. Xian, "Tracking control for robot manipulators with kinematic and dynamic uncertainty," *Int. J. Robot. Autom.*, vol. 23, no. 2, pp. 117–126, 2008.
[37] J. Xi, M. He, H. Liu, and J. Zheng, "Admissible output consensualization control for singular multi-agent systems with time delays," *J. Franklin Inst.*, vol. 353, no. 16, pp. 4074–4090, Nov. 2016.
[38] J. Xi, Z. Fan, H. Liu, and T. Zheng, "Guaranteed-cost consensus for multiagent networks with Lipschitz nonlinear dynamics and switching topologies," *Int. J. Robust Nonlinear Control.*, vol. 28, no. 7, pp. 2841–2852, 2018.
[39] J. Xi, C. Wang, H. Liu, and Z. Wang, "Dynamic output feedback guaranteed-cost synchronization for multiagent networks with given cost budgets," *IEEE Access*, vol. 6, pp. 28923–28935, 2018.
[40] J. Xi, C. Wang, H. Liu, and L. Wang, "Completely distributed guaranteed-performance consensualization for high-order multiagent systems with switching topologies," *IEEE Trans. Syst., Man, Cybern., Syst.*, to be published, doi: 10.1109/TSMC.2018.2852277.

ZHAOYING LI received the B.E. degree in detection guidance and control and the Ph.D. degree in aerospace engineering from Beihang University, Beijing, China, in 2005 and 2011, respectively. In 2008, she was a Visiting Student with the Department of Aerospace Engineering, Iowa State University. Since 2011, she has been with the School of Astronautics, Beihang University, where she is currently a Lecturer. Her research interests include flight control, path planning, and trajectory optimization.

WENJIE ZHOU received the B.S. degree in automation from Henan Polytechnic University, Henan, China, in 2015, and the M.E. degree in guidance, navigation, and control from Beihang University, Beijing, China, in 2018. His research interest is primarily in robust control, flight control, and quadrotor control.

HAO LIU (S'13–M'14) received the B.E. degree in control science and engineering from Northwestern Polytechnical University, Xi'an, China, in 2008, and the Ph.D. degree in automatic control from Tsinghua University, Beijing, China, in 2013. In 2012, he was a Visiting Student with the Research School of Engineering, The Australian National University. Since 2013, he has been with the School of Astronautics, Beihang University, Beijing, where he is currently an Associate Professor. He has also been with The University of Texas at Arlington Research Institute, Fort Worth, USA. His research interests include formation control, reinforcement learning, robust control, nonlinear control, unmanned aerial vehicles, unmanned underwater vehicles, and multi-agent systems. He received the Best Paper Award on IEEE ICCA 2018. He serves as an Associate Editor of the TRANSACTIONS OF THE INSTITUTE OF MEASUREMENT AND CONTROL.

LIXIN ZHANG received the B.S. degree in guidance, navigation, and control from Beihang University, Beijing, China, in 2016, where he is currently pursuing the M.E. degree with the School of Astronautics. His research interest is primarily in robust control, nonlinear control, and unmanned aerial vehicle control.

ZONGYU ZUO (M'14–SM'18) received the B.Eng. degree in automatic control from Central South University, Hunan, China, in 2005, and the Ph.D. degree in control theory and applications from Beihang University, Beijing, China, in 2011. He was an Academic Visitor with the School of Electrical and Electronic Engineering, The University of Manchester, from 2014 to 2015, and held an inviting Associate Professorship in mechanical engineering and computer science with UMR CNRS 8201, Université de Valenciennes et du Hainaut-Cambrésis, in 2015 and 2017. He is currently an Associate Professor with the School of Automation Science and Electrical Engineering, Beihang University. His research interests are in the fields of nonlinear system control, control of UAVs, and coordination of multi-agent system. He serves as an Associate Editor of the *International Journal of Aeronautical & Space Sciences*, and the *International Journal of Digital Signals and Smart Systems*.